

Supporting information for

Utilizing modeling, experiments, and statistics for the analysis of water-splitting photoelectrodes

Yannick K. Gaudy¹ and Sophia Haussener^{1,*}

¹ Institute of Mechanical Engineering, École Polytechnique Fédérale de Lausanne, 1015 Lausanne, Switzerland

Boundary conditions

Majority current – For a majority current, i.e an electron current in the case of an n-type material, the applied potential dropped in the SCR and HL, and, consequently, $\Delta\phi_H$ is not equal to zero. We developed a simple analytical solution presented below to determine $\Delta\phi_H$ depending on the applied potential.

A constant difference between the conduction band and Fermi level over the applied potential is assumed. The current densities in eqs. (20) and (21) are rewritten in terms of the potential difference in the SCR, $\Delta\phi_{sc}$:

$$\mathbf{i}_n \cdot \hat{\mathbf{n}} = -qv_{s,n}n_{eq}(e^{-\Delta\phi_{sc}/V_{th}} - 1) = -i_n^0(e^{-\Delta\phi_{sc}/V_{th}} - 1), \quad (S1)$$

$$\mathbf{i}_p \cdot \hat{\mathbf{n}} = qv_{s,p}p_{eq}(e^{\Delta\phi_{sc}/V_{th}} - 1) = i_p^0(e^{\Delta\phi_{sc}/V_{th}} - 1), \quad (S2)$$

where the electron and hole dark current densities are defined as $i_n^0 = qv_{s,n}n_{eq}$ and $i_p^0 = qv_{s,p}p_{eq}$. Note that the current densities shown in eqs. (S1) and (S2) are similar to valence and conduction band currents derived from Marcus theory or quantum mechanical theory for weak interactions¹.

In the case of majority current in an n-type semiconductor material, the band bending is negative ($\Delta\phi_{sc} < 0$) and the hole current negligible. If we assume $\Delta\phi_{sc} < -0.12V$, the total current given by the electron current density in eq. (S1) can be rewritten by:

$$\mathbf{i}_n \cdot \hat{\mathbf{n}} = i_{sc} = -i_n^0 e^{-\Delta\phi_{sc}/V_{th}}. \quad (S3)$$

Less than 1% error in the current appears when using this equation at $\Delta\phi_{sc} = -0.12V$ and the error decreases exponentially for smaller potentials (<0.05% error at $\Delta\phi_{sc} = -0.2V$).

With the current conservation presented in eq. (22), the current in the electrolyte must be equal to the current in the semiconductor at steady-state operation. The corresponding current in the electrolyte follows a Butler-Volmer equation and in terms of an HL potential difference, $\Delta\phi_H$, is given by^{2,3}:

* Corresponding author. E-mail address: sophia.haussener@epfl.ch, tel.: +41 21 693 3878.

$$i_H = i_{H_2}^0 \left(e^{\frac{(1-\alpha)\Delta\phi_H}{V_{th}}} - e^{-\frac{\alpha\Delta\phi_H}{V_{th}}} \right). \quad (S4)$$

In the case of n-type GaN and downward band bending, the exchange current density is the hydrogen evolution reaction exchange current density, $i_{H_2}^0$. The charge transfer coefficient, α , is typically around $\alpha \approx 0.5$ ². It should be noted that eq. (S4) does not take redox species concentration into account as we consider an electrolyte with high conductivity and without mass transport limitation. For downward band bending, the HL potential drop is negative and the anodic current becomes quickly negligible (<1% error on the current density at $\Delta\phi_H = -0.06V$) and eq. (S4) can be rewritten as a Tafel equation²:

$$i_H = -i_{H_2}^0 e^{-\frac{\alpha\Delta\phi_H}{V_{th}}}. \quad (S5)$$

With the current conservation (eq. (22)) and the potential drop equality (eq. (29)), the HL potential difference in case of downward band bending was given in terms of an applied potential by:

$$\Delta\phi_H(V_a) = \frac{V_{th} \ln\left(\frac{i_{H_2}^0}{i_n^0}\right) + V_a}{1+\alpha} < 0. \quad (S6)$$

The applied potential has to be at least below -0.18V according to eq. (29) and with $\Delta\phi_{sc} < -0.12V$ and $\Delta\phi_H < -0.06V$.

Experimental details

All measured potentials against Ag/AgCl sat. KCl were converted to the reversible hydrogen electrode (RHE) according to the Nernst equation⁴:

$$E_{RHE} = E_{Ag/AgCl} + 0.059\text{pH} + E_{Ag/AgCl}^0 \quad (S7)$$

where E_{RHE} is the converted potentials vs. RHE, $E_{Ag/AgCl}$ is the experimentally measured potential of Ag/AgCl sat. KCl and $E_{Ag/AgCl}^0$ is the potential of Ag/AgCl vs the standard hydrogen electrode (SHE) and equals +0.197V at 25°C⁵. An aqueous electrolyte of 1 M H₂SO₄ (pH=0) was used as the electrolyte.

The spectral irradiance of the UV LED used as a light source is depicted in Figure S1.

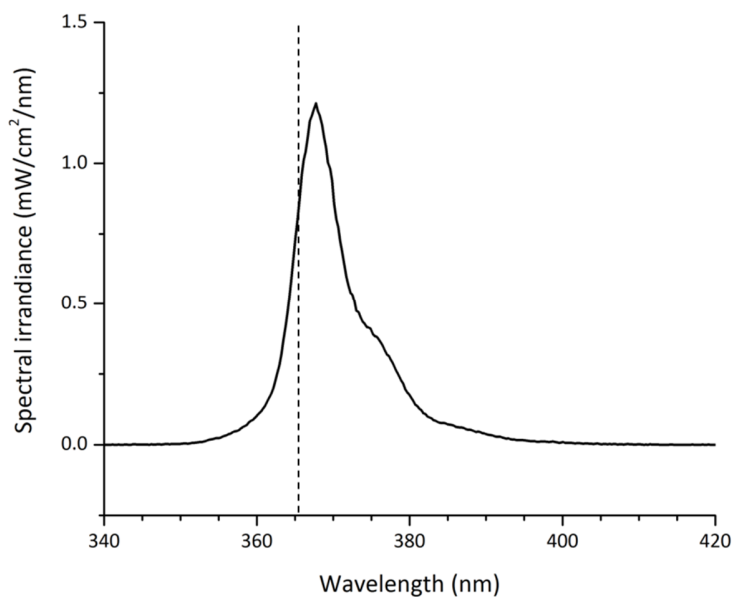


Figure S1 Spectral irradiance of the UV LED used for the experimental measurements. Only the part of the LED spectrum below 365.6nm is actually absorbed by GaN (dashed line).

The photocurrents were stable for the first few runs of cyclic voltammetry (6min) as depicted in Figure S2 before seeing the effect of photocorrosion.

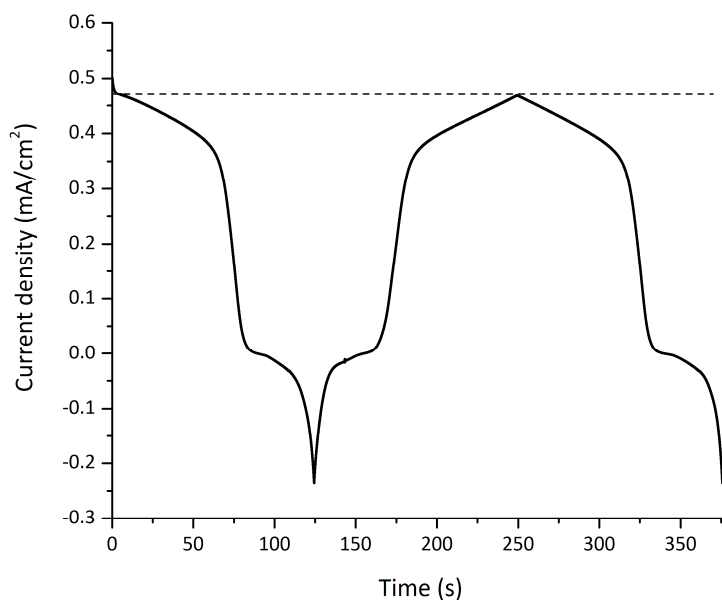


Figure S2 Current density versus time during linear sweep voltammetry. Potential sweep from 1.7V to -0.8V vs RHE. The dashed line indicates the current density at $t = 0$.

Numerical model – detailed results

For the reference cases (parameters indicated in Tables 1 and 2), the electron-hole pair generation rate in the semiconductor is depicted in Figure S3. The generation rate profile follows an exponential decrease similarly to the Beer-Lambert's law.

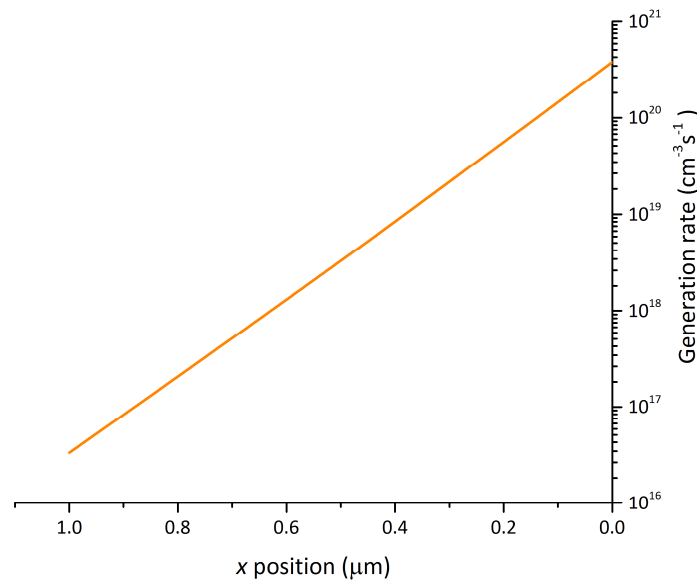


Figure S3 Numerical results of the electron-hole pair generation rate inside the semiconductor. The right side at 0μm is the illuminated side with the semiconductor-electrolyte interface and the left side at 1μm is the ohmic back contact (according to Figure 1).

The depth-dependent electron and hole concentration in the semiconductor at a potential of 0V vs RHE is depicted in Figure S4. At the ohmic contact ($x=1\mu\text{m}$), the hole concentration is zero because GaN is naturally n-doped and the ohmic contact assumes local thermodynamic equilibrium. The electron concentration equals the doping concentration $4\cdot 10^{16}\text{cm}^{-3}$ in the bulk of the semiconductor according to Poisson's equation (see eq.(4)), since the charge density is zero and the hole concentration is negligible as depicted in Figure S4. In the space charge region, the electron concentration drops while the hole concentration increases as depicted in Figure S5. The hole concentration is higher than the electron concentration at the semiconductor-electrolyte interface ($x=0$) and therefore the minority current dominates at the interface.

The band potential diagram at a potential of 0V vs RHE is depicted in Figure S5. The quasi-Fermi potentials are split inside the entire semiconductor due to the generation rate profile inside the semiconductor (see Figure S3) and because n-doped GaN does not contain any acceptors. The quasi-Fermi potentials only unite at the ohmic contact where there is thermodynamic equilibrium.

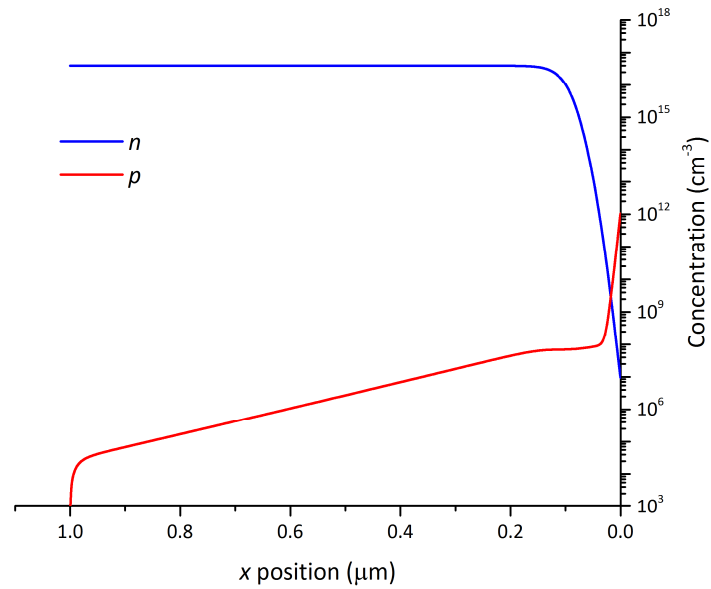


Figure S4 Numerical results of the electron (blue line) and hole (red line) concentration at 0V vs RHE inside the semiconductor. The right side at 0 μm is the illuminated side with the semiconductor-electrolyte interface and the left side at 1 μm is the back ohmic contact (according to Figure 1).

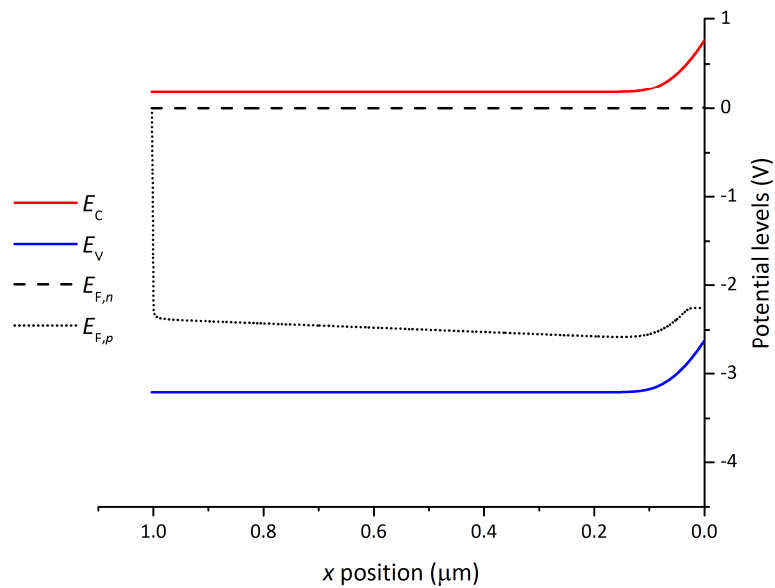


Figure S5 Numerical results of the band potential diagram at 0V vs RHE with conduction band (red line), valence band (blue line), electron and hole quasi-Fermi potential (dashed and dotted lines respectively) inside the semiconductor. The right side at 0 μm is the illuminated side with the semiconductor-electrolyte interface and the left side at 1 μm is the back ohmic contact (according to Figure 1).

Parametric analysis on key factors

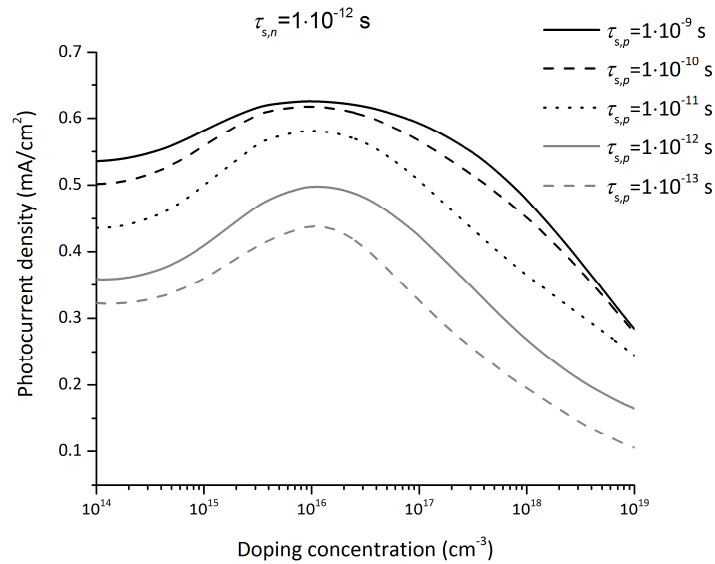


Figure S6 Photocurrent density at 1.23V vs RHE as a function of the doping concentration for various hole surface lifetimes ($\tau_{s,p} = 10^{-9}, 10^{-10}, 10^{-11}, 10^{-12}, 10^{-13}$ s) and an electron surface lifetime of 1ps. An optimum doping concentration appeared at $1 \cdot 10^{16}$ cm⁻³.

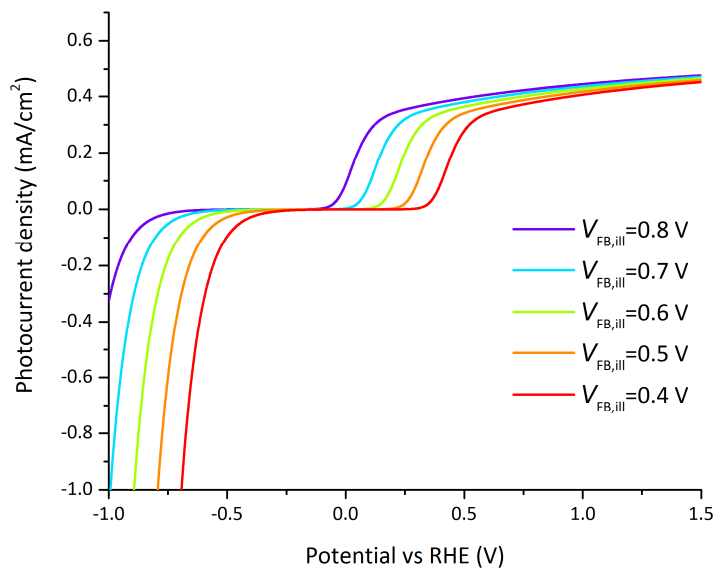


Figure S7 Photocurrent-voltage curves for varying flatband potentials for the reference case (parameters indicated in Tables 1 and 2).

References

- 1 R. Memming, *Semiconductor Electrochemistry*, Wiley-VCH, Weinheim, 2001.
- 2 A. J. Bard and L. R. Faulkner, *Electrochemical Methods: Fundamentals and Application*, John Wiley & Sons, Inc., Second edi., 2001.
- 3 J. Newman and K. E. Thomas-Alyea, *Electromchemical Systems*, John Wiley & Sons, Inc., 3rd editio., 2001.
- 4 X. Qi, G. She, X. Huang, T. Zhang, H. Wang, L. Mu and W. Shi, *Nanoscale*, 2014, **6**, 3182–9.
- 5 A. J. Bard, L. R. Faulkner, E. Swain and C. Robey, *Fundamentals and Applications*, .